Time-resolved measurements of the angular distribution of the Ni-like Pd soft-x-ray laser emission

C. Imesch, F. Staub, and J. E. Balmer
Institute of Applied Physics, Sidlerstrasse 5, 3012 Bern, Switzerland
(Received 1 October 2007; published 12 June 2008)

The temporal history of the x-ray laser output has been measured in dependence of the emission angle of the x-ray laser with respect to the target plane. The results show both the exit time (the time at which the x-ray laser pulse is leaving the plasma) and the pulse duration to depend on the angle of emission. Simulations of the gain in Ni-like Pd combined with ray tracing through the plasma were used to model the dependence of the time of emission on the deflection angle of the individual rays within the laser emission cone. The simulations are in reasonable agreement with the measurements.

DOI: 10.1103/PhysRevA.77.063818 PACS number(s): 42.55.Vc, 78.47.−p

I. INTRODUCTION

Rapid progress in the development of collisionally pumped soft-x-ray lasers in recent years has lead to a number of robust saturated lasing lines using the Ne-like (e.g., Zn, Ge, Se, etc.) and Ni-like (e.g., Pd, Ag, Sn, etc.) schemes. The output properties of these lasers have been characterized in terms of the most relevant laser parameters including output energy, pulse duration, coherence, near-field and far-field energy distributions, and divergence [1–4]. In addition to this, time-resolved measurements of the x-ray laser emission will help to improve our understanding of the plasma dynamics and atomic level population mechanisms [5–10]. In recent work by our group, experiments aimed at measuring the absolute timing of the x-ray laser output with respect to the arrival of the drive pulse were presented [11].

Further insight into the temporal evolution of the plasma parameters can be gained from time-resolved measurements of the angular distribution of the x-ray laser emission. Measurements showing the emission angle to vary during the pulse were reported for Ne-like lasers [12,13]. As the duration of the drive pulse was relatively long (700 ps) in these experiments, the observed change of the emission angle with time was attributed to a decrease of the density gradient during laser emission. Similar results were reported in [14] for the Ni-like Sm laser for the case of 75-ps drive pulse duration.

In this work we describe our recent experiments aimed at measuring the time dependence of the x-ray laser emission angle in Ni-like Pd, combined with numerical simulations for the case of 100-ps drive pulse duration.

II. EXPERIMENTAL SETUP

The experiments were performed using the 1054-nm Nd:glass laser system at the Institute of Applied Physics of the University of Bern. The laser, having a final amplifier of 90-mm diameter, is capable of delivering up to 30 J at a pulse duration of 100 ps [full width at half maximum (FWHM)]. The output beam was focused to give a line focus of 2.5-cm length and approximately 80-μm width using a combination of a 500-mm focal length aplanatic doublet and a −1700-mm focal length cylindrical lens. Targets were 25-mm wide slabs having a diamond-machined surface finish. A 0.5% prepulse irradiated the target 5 ns before the arrival of the main pulse. With these settings, the x-ray laser output was found to be saturated with a gain-length product of ~17 in previous work [15].

The time-resolved diagnostics setup is shown in Fig. 1. The x-ray laser emission is directed onto the 140-μm wide slit of a Kentech ×2-magnification x-ray streak camera via a 1200-lp/mm aberration-corrected flat-field Hitachi grating. The slit of the streak camera is oriented parallel to the angularly dispersed 14.7-nm Pd lasing line, so that the streak camera produces a time-vs-emission angle image of the x-ray pulse. The 140-μm slit is matched in width to the resolution of the streak camera and allows the x-ray laser line to pass undisturbed. The streak camera is equipped with a transmission photocathode made up of a 200-Å thick layer of aluminum deposited on a 1200-Å thick Formvar foil.

The streaked signal is read out by an image intensifier coupled to a cooled charge-coupled device (CCD) camera (Photometrics STAR I) having a pixel size of 23 μm. To avoid saturation of the streak camera, a 10-μm wide slit and several Al-on-Formvar filters were inserted at the entrance of the spectrograph [11]. The (instrumental) time resolution of the streak camera was ~15 ps, as calculated from the sweep speed (previously calibrated [11]), the width of the streak slit, the velocity distribution of the secondary electrons and the magnification. Although the time resolution is not very high, it is sufficient for our measurements, as the measured pulse durations were always over ~30 ps.

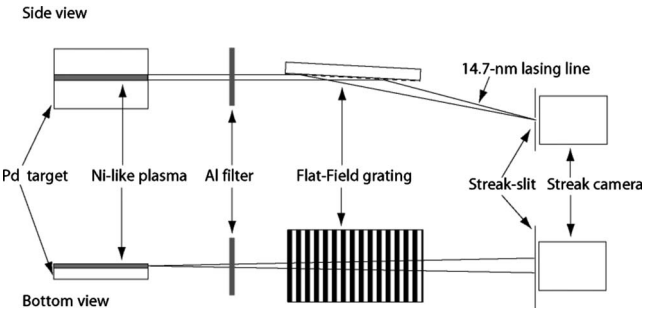

FIG. 1. Side and bottom view of the setup for time-resolved measurements of the beam angular distribution.

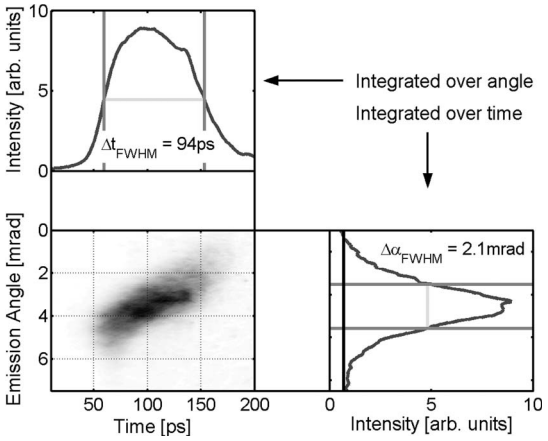

FIG. 2. Time- and angle-resolved x-ray laser emission from the Pd lasing line. At the top is the temporal trace and on the right side is the angular trace. The zero points of the axes were chosen arbitrarily. The zero point of the angular axis was shifted to match the simulation (see Fig. 7).

III. EXPERIMENTAL RESULTS

The measurements were performed at main pulse energies between 22 and 26.5 J (corresponding to irradiances between 11 and 13.3 TW/cm^2). A typical recording of the streak camera is shown in Fig. 2. The picture shows that the deflection angle varies with time. Its value is largest at the beginning of the x-ray laser emission and then decreases continuously until the end of the emission, i.e., the x-ray laser beam sweeps in time towards the target surface.

A series of shots such as that shown in Fig. 2 were analyzed in the following way: First, the FWHM's over time and divergence of the x-ray laser pulses were computed by integration over the divergence and time domain, respectively (Fig. 2, top and right) and plotted in Fig. 3. The results of all the measurements were found to lie in the range between 2.1 to 2.5 mrad and 71 to 98 ps, except for two shots. The mean values are 2.4 ± 0.7 mrad for the deflection angle and 82 ± 14 ps for the total pulse duration.

Secondly, the pulse duration $\Delta t_{\mathrm{FWHM}}(\alpha)$ was extracted as a function of the deflection (viz. observation) angle and plotted in Fig. 4. We note that this corresponds to the usual setup for time-resolved measurements with the slit of the streak camera oriented parallel to the target surface. As a function of the emission angle, the pulse duration is seen to vary from ~40 ps at the edges of the beam to ~65 ps in the angular center of the beam (measurement points in Fig. 4). The average pulse width is 50 ± 11 ps. This is in good agreement with our previous work [11], where a value of 47 ± 11 ps was obtained. One important consequence of this is that "conventional" time-resolved measurements are inherently inaccurate in the sense that they do not provide the full x-ray laser emission duration, but only the duration within an angular slice of the beam.

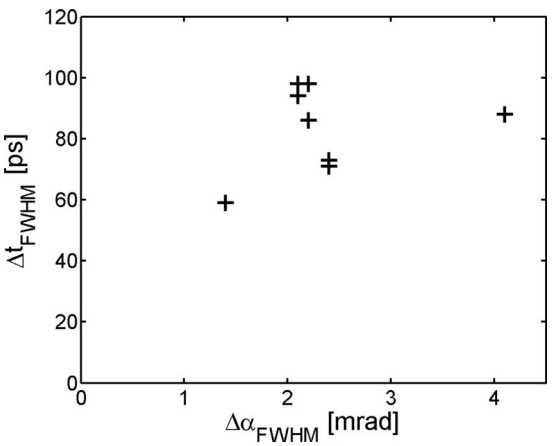

FIG. 3. Relation between the divergence angle and the duration of the pulse.

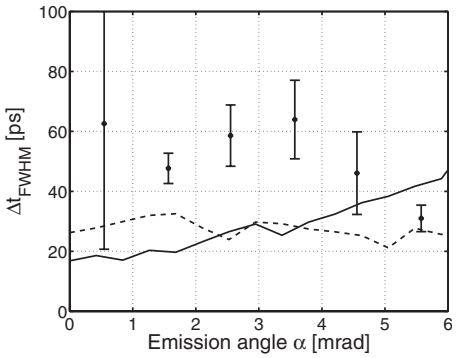

FIG. 4. Comparison of the angle-dependent pulse width $\Delta t_{\mathrm{FWHM}}(\alpha)$ obtained from the measurements (dots) and the simulations using standard irradiance (dashed line, cf. Fig. 7) and reduced irradiance (solid line, cf. Fig. 9). The dots are the average of several different shots with standard deviations visualized by the error bars.

IV. NUMERICAL RESULTS

In order to model the experiments, a ray-tracing code was combined with the temporal and spatial evolution of the gain obtained from simulations using the LASNEX and CRETIN codes reported in previous work [11].

Figure 5 shows the x-ray laser propagation paths through the plasma along the line focus for three selected rays. The full fan of rays was chosen in order to match the distance of the emission region from the target (~70 μm) with previous results [4]. The electron density distribution used for the ray tracing was extracted from the simulation at a time 60 ps

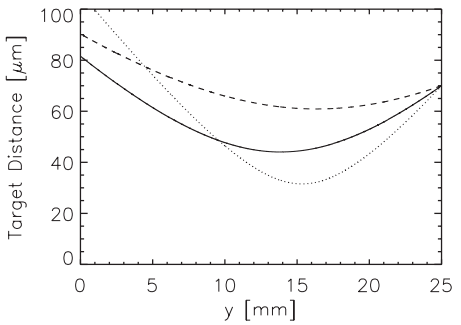

FIG. 5. Ray-tracing paths for three different deflection angles (2, 4, and 6 mrad).

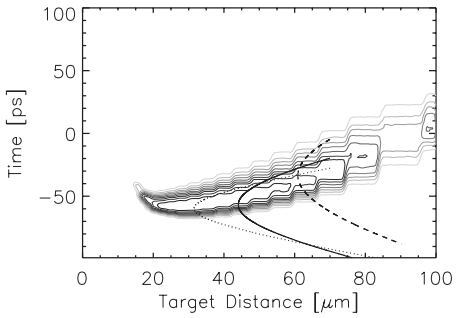

FIG. 6. Calculated temporal and spatial evolution of the gain for the Ni-like Pd line for an incident pump irradiance of 10 TW/cm^2 using a 0.5% prepulse at 5 ns delay. The three ray paths are the same as in Fig. 5. The initial time of each ray was chosen in order to achieve maximum gain-length product. A contour line corresponds to 10 cm^{-1}.

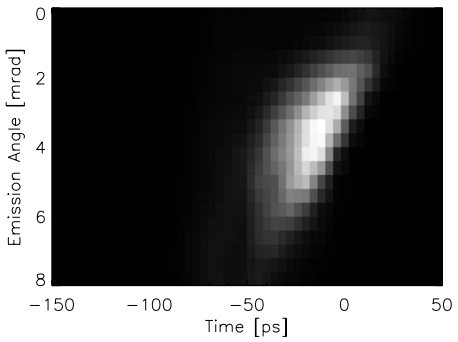

FIG. 7. Simulated pulse shape using the gain map of Fig. 6.

before the peak of the pump pulse, where the peak of the x-ray laser emission was measured in our previous work. In Fig. 5, the deflection angle of the central ray (solid) is 4 mrad, the marginal rays have angles of 2 mrad (dashed) and 6 mrad (dotted), respectively.

Figure 6 shows, in the form of a contour plot, the simulated temporal and spatial evolution of the gain (gain map) for the nickel-like palladium line in the case of a 0.5% prepulse preceding the 10-TW/cm^2 main pulse by 5 ns. The horizontal axis gives the distance in microns from the target surface while the vertical axis gives the time in picoseconds with 0 ps representing the peak of the 100-ps drive pulse. As can be seen, the region of maximum gain appears before the peak of the main pumping pulse, which is in good agreement with results from [8,9,11]. Also shown are the three rays from Fig. 5 (discrete curves) for which the path distance y along the line focus has been expressed in terms of its propagation time. In the gain plot the three rays are shifted in time such as to maximize the gain-length product along each path, i.e., the temporal position of the rays represents the instant of the peak contribution at the particular emission angle to the total x-ray laser emission. As can be seen, the rays do not propagate in the gain region at constant distance from the target (parallel to the time axis), but are refracted away from the target, partially following the gain zone in time and space. This leads to an increased effective gain duration, as a considerable fraction of the length of the plasma column contributes to the gain-length product. The effect of gain saturation was found to additionally increase the pulse duration and was taken into account for the calculation. Also taken into account was the backward beam, which influences the saturation behavior of the measured forward beam [16]. The temporal extent of the ray fan was taken as 83 ps, which corresponds to the transit time along the 25-mm plasma column. As can be seen, the ray exhibiting the largest deflection angle penetrates deepest into the plasma and follows the gain region along the highest gain values after the turning point. The midray shows a slightly longer path through the gain region, but travels through zones of more moderate gain and reaches its peak gain-length product later in time. The path of the ray being emitted with the smallest deflection angle only sees small values of gain and is being emitted latest in time.

Numerical integration of the resulting x-ray laser output leads to Fig. 7 and simulation No. 1 in Table I. Consistent with the experiment, the x-ray laser peaks earlier in time for higher deflection angles than for rays suffering less refraction in the plasma, with a global peak in intensity around the central ray, which is being emitted at 4 mrad. The time-integrated divergence of the simulation is $\Delta\alpha_{\mathrm{FWHM}}=3.7$ mrad, and the angle-integrated pulse duration $\Delta t_{\mathrm{FWHM}}=39$ ps, which differs significantly from the measurements. The calculated angle-dependent pulse duration $\Delta t_{\mathrm{FWHM}}(\alpha)$ is found to be approximately constant in the range of 25–30 ps (dashed line in Fig. 4). However, the slope $\Delta\alpha/\Delta t$ of the pulse shape in time versus the emission angle (Fig. 7) is much higher than for the measurement in Fig. 2.

There are several issues that are not modeled correctly by this simulation. Experimentally, the peak of the x-ray laser emission was observed at a distance of ~70 μm from the target surface [4], while the simulation predicts increasing x-ray fluence with distance, as the calculated gain region reaches out to a distance of 100 μm from the target. This effect can be attributed to the lack of a rigorous consideration of two-dimensional plasma expansion, which is only partially accounted for by an expansion angle of 15° in the lateral direction. However, due to the long delay of 5 ns between prepulse and main pulse, two-dimensional expansion effects are to be expected, which modify the gain region at long distances from the target in a way that the gain drops due to the rapidly decreasing electron density and temperature.

A second point is that the irradiance of the pump laser decreases towards the ends of the line focus. Reduced irradiance leads to decreasing temperature, ionization, and gain

TABLE I. Results of the measurements and simulations of the temporally and angularly resolved Pd x-ray laser emission. The rows contain the FWHM of the emission angle $\Delta\alpha$ and the pulse duration Δt, the slope $\Delta\alpha/\Delta t$, and the corresponding figure number.

	No.	$\Delta\alpha_{\mathrm{FWHM}}$ (mrad)	Δt_{FWHM} (ps)	$\Delta\alpha/\Delta t$ (μrad/ps)	Figure
Measured		2.4	82	35	2
Simulated	1	3.7	39	80	6 and 7
Simulated	2	3.4	43	53	8 and 9

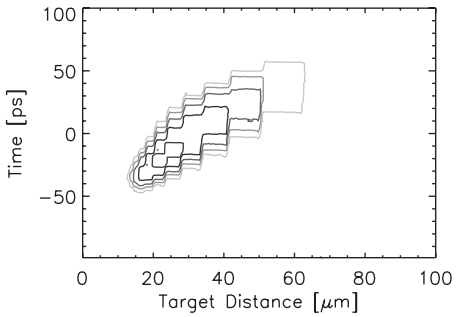

FIG. 8. Calculated temporal and spatial evolution of the gain for the Ni-like Pd line for an incident pump irradiance of 2 TW/cm^2 using a 0.5% prepulse at 5 ns delay. A contour line corresponds to 6 cm^{-1}.

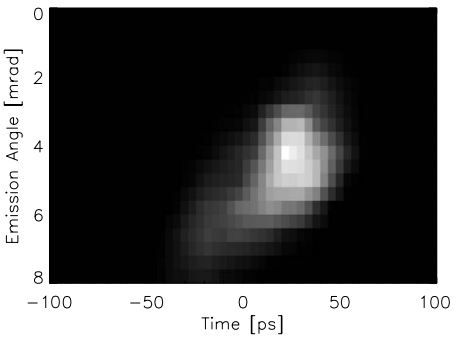

FIG. 9. Simulated pulse shape using the gain of Fig. 8.

as well as to a reduced velocity at which these observables are taken along within the expanding plasma. This causes the effective gain region to be modified towards the ends of the line focus due to decreasing irradiance. With respect to Fig. 6, this means that towards the ends of the line focus the gain region remains closer to the target surface. The net effect is a narrowed gain region leading to smaller divergence, a reduced slope $\Delta\alpha/\Delta t$, and a peak emission shifted towards the target surface as compared to the idealized simulation. However, simulations including a nonconstant intensity along the line focus showed an effect too small to account for the discrepancy with the measurements.

An improved match to the measurements was obtained with a simulation performed for a pump irradiance of 2 TW/cm^2. The corresponding result of the LASNEX/CRETIN gain simulation is shown in Fig. 8. The resulting ray-tracing simulation is shown in Fig. 9. It reveals a considerably smaller slope $\Delta\alpha/\Delta t$ (cf. Table I, simulation No. 2) and shows a reasonable agreement with the measured time dependence of Fig. 2. The improved agreement at lower pump energy may be explained by incomplete absorption of the incident pump light in the plasma and is not clearly understood [17].

Compared to the measurements the temporal extent of the simulation still shows a stronger dependence of the emission angle on time with a slope $\Delta\alpha/\Delta t=53$ μrad/ps (Fig. 9), while the experimental results show a slope of only 35 μrad/ps. The divergence $\Delta\alpha$ of the emission was measured to be roughly 70% of the value found in the simulation. An overview of the simulation results and the measurements can be found in Table I.

V. DISCUSSION

In a first step the electron density distribution in the ray tracing was assumed to be constant during the gain duration. The evolution of the gain, however, was calculated with full time dependence. As the propagation speed of the gain zone is much faster than the plasma expansion, the spatial movement and expansion of the gain zone with time plays the major role on the decrease of the density gradient. The gain duration is too short for the density gradient to relax appreciable. As the gain region moves away from the target towards less dense plasma, the refraction within the gain zone decreases primarily due to the propagation of the gain region towards less refractive plasma, and not due to a relaxation of the density gradient itself.

Although the time variation of the electron density caused by the gradient relaxation is negligible, the density can increase in time through additional ionization by the main pulse, changing the value of the refractive index of the plasma as a function of time. To simulate this, we multiply the original electron density distribution with a time dependent factor, such that $n_e(t)=a(t)n_{e0}$. $a(t)$ is a factor that is taken to vary linearly in time with $n_{e0}=1.2\times10^{20}$ cm^{-3} at a distance of 50 μm from the target. The result is that even in the case of a factor-of-4 change in electron density both the position of the emission angle and the pulse duration Δt_{FWHM} remain essentially unaltered. The main effect is an increase in the divergence $\Delta\alpha_{\mathrm{FWHM}}$ with increasing electron density.

VI. CONCLUSIONS

Measurements of the temporally resolved angle of emission of the Pd x-ray laser were presented and compared with numerical simulations. The angle of emission was seen to vary with time, with the highest deflection angles being emitted first. Numerical simulations show that the angular variation of the x-ray laser emission is a consequence of the propagation of the x-ray photons through the spatiotemporally evolving gain zone. For a good quantitative match, a reduced irradiance of the pump laser had to be assumed in the simulations.

ACKNOWLEDGMENTS

The authors would like to thank B. Locher for expert technical assistance, and W. Lüscher for target preparation. This work was supported in part by the Swiss National Science Foundation.

[1] J. Zhang *et al.*, Phys. Rev. Lett. **78**, 3856 (1997).
[2] J. Nilsen *et al.*, Phys. Rev. A **56**, 3161 (1997).
[3] J. Y. Lin *et al.*, Opt. Commun. **158**, 55 (1998).
[4] C. Siegel, M. Braud, J. E. Balmer, and J. Nilsen, Opt. Commun. **210**, 305 (2002).
[5] J. Nilsen, J. C. Moreno, B. J. MacGowan, and J. A. Koch, Appl. Phys. B: Photophys. Laser Chem. **57**, 309 (1993).
[6] P. Lu, Y. Li, and E. E. Fill, Phys. Rev. A **54**, 5193 (1996).
[7] H. Daido *et al.*, Opt. Lett. **20**, 61 (1995).
[8] J. Nilsen and J. C. Moreno, Opt. Lett. **20**, 1386 (1995).
[9] H. Daido, Y. Kato, K. Murai, S. Ninomiya, R. Kodama, G. Yuan, Y. Oshikane, M. Takagi, H. Takabe, and F. Koike, Phys. Rev. Lett. **75**, 1074 (1995).
[10] J. Kuba *et al.*, J. Phys. IV **11**, PR2-43 (2001).
[11] F. Staub, M. Braud, J. E. Balmer, and J. Nilsen, Phys. Rev. A **72**, 043813 (2005).
[12] R. Kodama *et al.*, Opt. Commun. **90**, 95 (1992).
[13] R. Smith *et al.*, CLF Annual Report 1996/97 (unpublished), p. 36ff.
[14] J. Zhang *et al.*, Science **276**, 1097 (1997).
[15] J. E. Balmer, M. Braud, and F. Loewenthal, J. Phys. IV **11**, PR2-137 (2001).
[16] G. J. Pert, J. Opt. Soc. Am. B **11**, 1425 (1994).
[17] R. E. King *et al.*, Phys. Rev. A **64**, 053810 (2001).